Novel approach based on GQD-PHB as anchoring platform for the development of SARS-CoV-2 electrochemical immunosensor

Gustavo Martins, Jeferson L. Gogola, Lucas H. Budni, Maurício A. Papi, Maritza A.T. Bom, Maria L.T. Budel, Emanuel M. de Souza, Marcelo Müller-Santos, Breno C.B. Beirão, Craig E. Banks, Luiz H. Marcolino-Junior, Márcio F. Bergamini

Abstract

In the present work, we report an innovative approach for immunosensors construction. The experimental strategy is based on the anchoring of biological material at screen-printed carbon electrode (SPE) modified with electrodeposited Graphene Quantum Dots (GQD) and polyhydroxybutyric acid (PHB). It was used as functional substract basis for the recognition site receptor-binding domain (RBD) from coronavirus spike protein (SARS-CoV-2), for the detection of *Anti*-S antibodies (AbS). SEM images and EDS spectra suggest an interaction of the protein with GQD-PHB sites at the electrode surface. Differential pulse voltametric (DPV) measurements were performed before and after incubation, in presence of the target, shown a decrease in voltametric signal of an electrochemical probe ($[Fe(CN)_6]^{3/4-}$). Using the optimal experimental conditions, analytical curves were performed in PBS and human serum spiked with AbS showing a slight matrix effect and a relationship between voltametric signal and AbS concentration in the range of 100 ng mL^{-1} and 10 µg mL^{-1}. The selectivity of the proposed sensor was tested against yellow fever antibodies (YF) and the selective layer on the electrode surface did not interact with these unspecific antibodies. Eight samples of blood serum were analyzed and 87.5% of these total investigated provided adequate results. In addition, the present approach showed better results against traditional EDC/NHS reaction with enhancements in time and the possibility to develop an immunosensor in a single drop, since the proteins can be anchored prior to the electrode modification step.

Keywords: Immunosensors construction, Carbon nanomaterial, Electrochemical devices

Graphical abstract

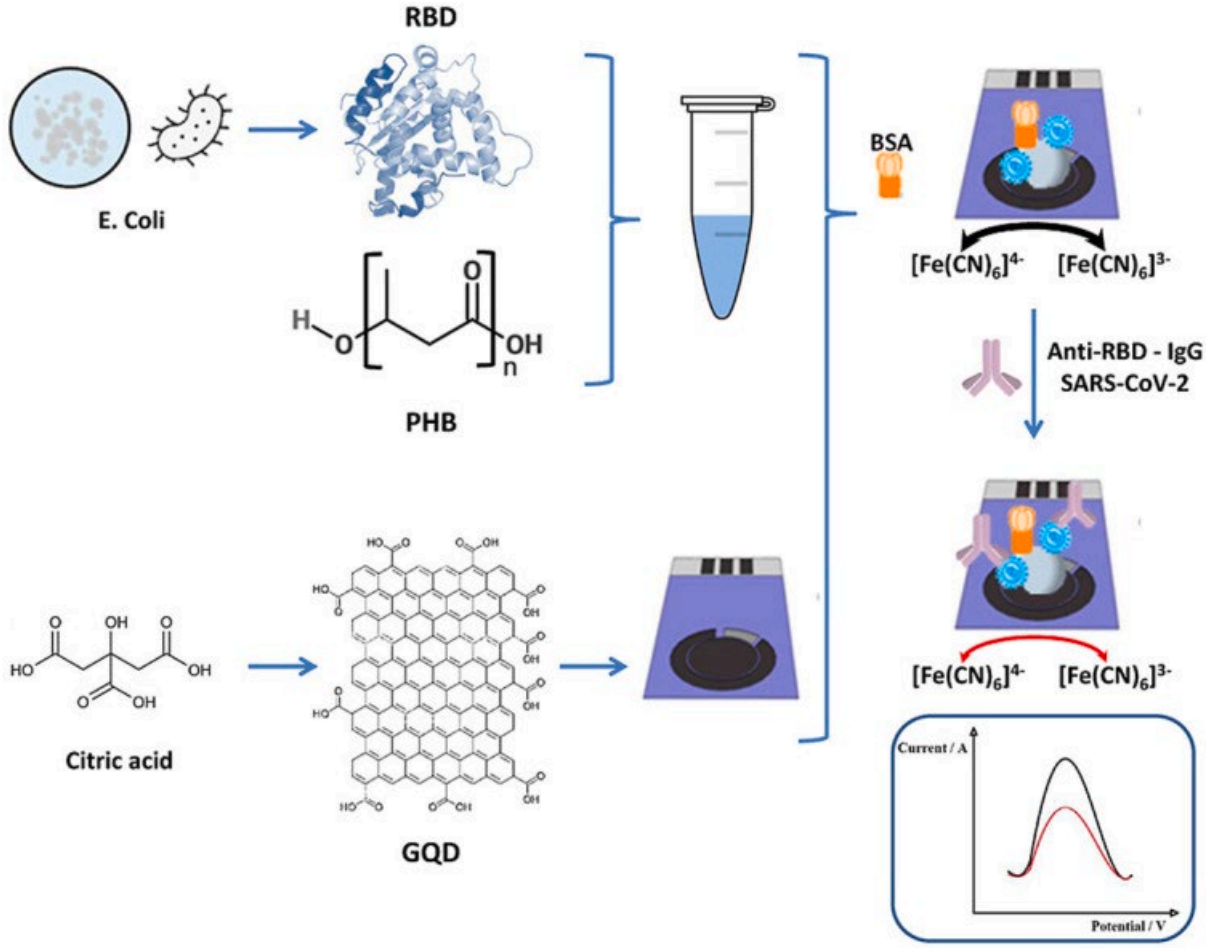

1. Introduction

The recent pandemic caused by Severe Acute Respiratory Syndrome Coronavirus 2 (SARS-CoV-2) showed how unprepared we are. Diagnosis sciences still in lack of a rapid, affordable, cheap and reliable diagnostic tests. Even with the globally coordinated research to respond to COVID-19 threats, a standard procedure to deal with the virus took some time to be set [1]. The gold-standard method for viral detection is a molecular diagnostic test aiming for viral RNA, using real time reverse transcriptase-polymerase chain reaction (RT-PCR). Frequently, RT-PCR assays are complemented by serological and immunological tests, such as indirect immunofluorescence test or enzymatic immunoassay (ELISA) [2,3]. On the other side, point-of-care (POC) devices such as lateral flow tests (LFT) are often alternatives for clinical trials, as they are cheap, rapid, and easy to use [[4], [5], [6]].

Electrochemical analyses are increasingly being used as rapid tests, since this methodology provides a straightforward and cheap arrangement due to the possibility of label-free detection [[7], [8], [9]]. In addition, the transducer can be modified with nanomaterials such as carbon nanotubes and graphene have been systematically explored as signal amplifiers [10]. Graphene Quantum Dots (GQD), a carbon-based nanomaterial, recently obtained great attention in the development of immunosensors. GQDs are small fragments of graphene sheets [11]. Thus, it shares graphene overall properties with enhancements on surface area, abundance of functional groups, ease of functionalization, higher biocompatibility and lower toxicity [[11], [12], [13]]. Therefore, GQD is a prosperous material for the development electrochemical immunosensors, specially point-of-care focused ones. Since, its synthesis can be performed by incomplete pyrolysis of citric acid, an easy and cheap approach [14].

Protein anchoring on carbon functionalized materials traditionally employs crosslinking reactions to activate its surface and covalently bind the protein to the carbon surface [15]. As an alternative, polyhydroxyalkanoates (PHA) spontaneously bind to protein residues. Specifically, polyhydroxybutyrate (PHB) allows the synthesis of a core-shell nanostructure (100–300 nm) with a hydrophobic core and a surface exposing binding domains, that allows protein interaction and binding [[16], [17], [18]]. Similarly, this anchoring system is suitable for biosensors construction and application, however poorly explored in the development of electrochemical biosensors [19,20].

For this purpose, electrochemical immunosensors combine the inherent specificity of immunoreactions with the high sensitivity of electrochemical sensors and thus sustain the development of the next generation of POC tests. Therefore, here we propose the development of an electrochemical immunosensor for the detection of SARS-CoV-2 antibodies based on bioengineered PHB and GQD as anchoring platforms on screen-printed electrodes.

2. Materials and methods

2.1. Materials and reagents

All chemicals were analytical or high-purity grade. *N*-(3-Dimethylaminopropyl)-*N*'-ethylcarbodiimidehydrochloride (EDC), *N*-Hydroxysuccinimide sodium salt (NHS), Potassium Ferricyanide $K_3[Fe(CN)_6]$ and citric acid were purchased from Sigma Aldrich. Phosphate buffer saline, pH 7.4, were prepared with sodium chloride, potassium chloride, potassium phosphate monobasic and disodium hydrogen phosphate all from Sigma Aldrich. Bovine serum album (BSA) and Antibody against Yellow Fever (YF - 0.16 mg mL^{-1}) were provided by Molecular Virology Laboratory at Carlos Chagas Institute – FIOCRUZ/PR.

The screen-printed electrodes (SPE) were obtained from Professor Craig E. Banks laboratory at Manchester Metropolitan University. Working and counter electrodes are made of graphite conductive ink, and an Ag|AgCl ink was used for the pseudo-reference electrode construction. The final set is supported on a polyester substrate with electrodes and electrical contacts delimited by an insulating ink.

Polyhydroxybutyrate particles were produced by the nanoprecipitation method [21]. 10 mg of PHB (Sigma Aldrich, #363502) was dissolved in 10 ml of TFE (2,2,2-trifluoroethanol) (Sigma Aldrich, #T63002) with stirring at room temperature. The solution was dialyzed through a 12 kDa cut-off cellulose membrane (Sigma Aldrich, #D9777) against 2 L of distilled water for 24 h.

2.2. Expression and purification of the recombinant RBD (receptor binding domain) from the SARS-CoV-2 spike protein

The amino acid sequence between the residues 319 to 541 from SARS-CoV-2 Spike protein (NCBI, Gene ID: 43740568) was codon-optimized and fused to the Substrate-Binding Domain (SBD) of PHA depolymerase of *Alcaligenes faecalis* [22] followed by a 6-histidines tag in the C-terminal. Twist Bioscience (South San Francisco, CA, USA) synthesized the synthetic construct on-demand and cloned it into the NdeI and XhoI sites of the pET29b(+), generating the pET29-RBD-SBD-6His. The 6-histidines tag was used to purify the protein by affinity chromatography against nickel (Ni^{2+}) ions. The SBD domain interacts with PHB as previously described [22].

E. coli BL21(DE3) carrying the pET29-RBD-SBD-6His was cultivated in 80 mL of Lysogeny Broth [23]. The concentration of RBD-SBD was measured by the Bradford method using BSA as standard [24]. For the sake of clearness, hereafter, we referred to RBD-SBD as RBD.

2.3. Electrochemical measurements

Cyclic voltammetry (CV), differential pulse voltammetry (DPV) and Electrochemical impedance spectroscopy (EIS) measurements were performed with SPE on a Potentiostat/Galvanostat PGSTAT204. Experiments were conducted in PBS 0.1 mol L^{-1}, pH 7.4, with 2.0 mmol L^{-1} of ($K_3[Fe(CN)_6]$) as the electrochemical probe. The progression of the proposed immunosensor was evaluated by the suppression anodic current peak after each anchoring step, since proteins are essentially nonconductors. EIS were performed with probe anodic peak potential and 10 mV amplitude.

2.4. Morphological and structural characterization

Scan electron microscopy (SEM) images were performed in a FEI High-Resolution Scanning Electron Microscope, Felmi ZFE - model Quanta 450, with a field emission gun (FEG) electron source, which has a resolution of 1.0 nm. All images were obtained with 10 kV voltage acceleration and secondary electron detectors. Elemental chemical analysis of EDS has resolution of 131 eV with a Apollo X SDD detector.

The Infrared spectra were obtained with a BOMEN spectrometer, 64 scans from 4000 cm^{-1} to 500 cm^{-1}. Samples were previously homogenized with KBr pastille and dried.

2.5. Immunosensor construction

First, GQD was electrodeposited on the SPE surface. This step was performed by CV throughout −1.4 to 0.0 V, 50 mV s^{-1}, 3 until 10 cycles. Afterwards, 2.0 µL of PHB particles solution was added directly to the working electrode (WE), and it was allowed to dry in controlled temperature (37 °C). Following this step, RBD was added (2.0 µL) to WE and incubated at 37 °C in a saturated water atmosphere, every incubation was performed under this condition. All incubation times were monitored, ranging from 15 min to 60 min. Sequently, electrodes were 3 times washed by immersion on PBS solution, in order to remove excess and not binded biomolecules, this step was repeated after each incubation. Next step consisted of block PHB residual active sites, that did not bind to RBD, in order to mitigate parallel interactions. This was performed by adding 2 µL of BSA (1.0 mg mL^{-1}) and incubating for 15 min at 37 °C. Finally, antibody detection (AbS) was done by adding and incubating 2 µL of AbS solution. Each step involving the construction of the sensor was evaluated by CV, −0.3 to 0.6 V, 50 mV s^{-1}, 3 cycles. Scheme 1 represents every step on building up the proposed sensor.

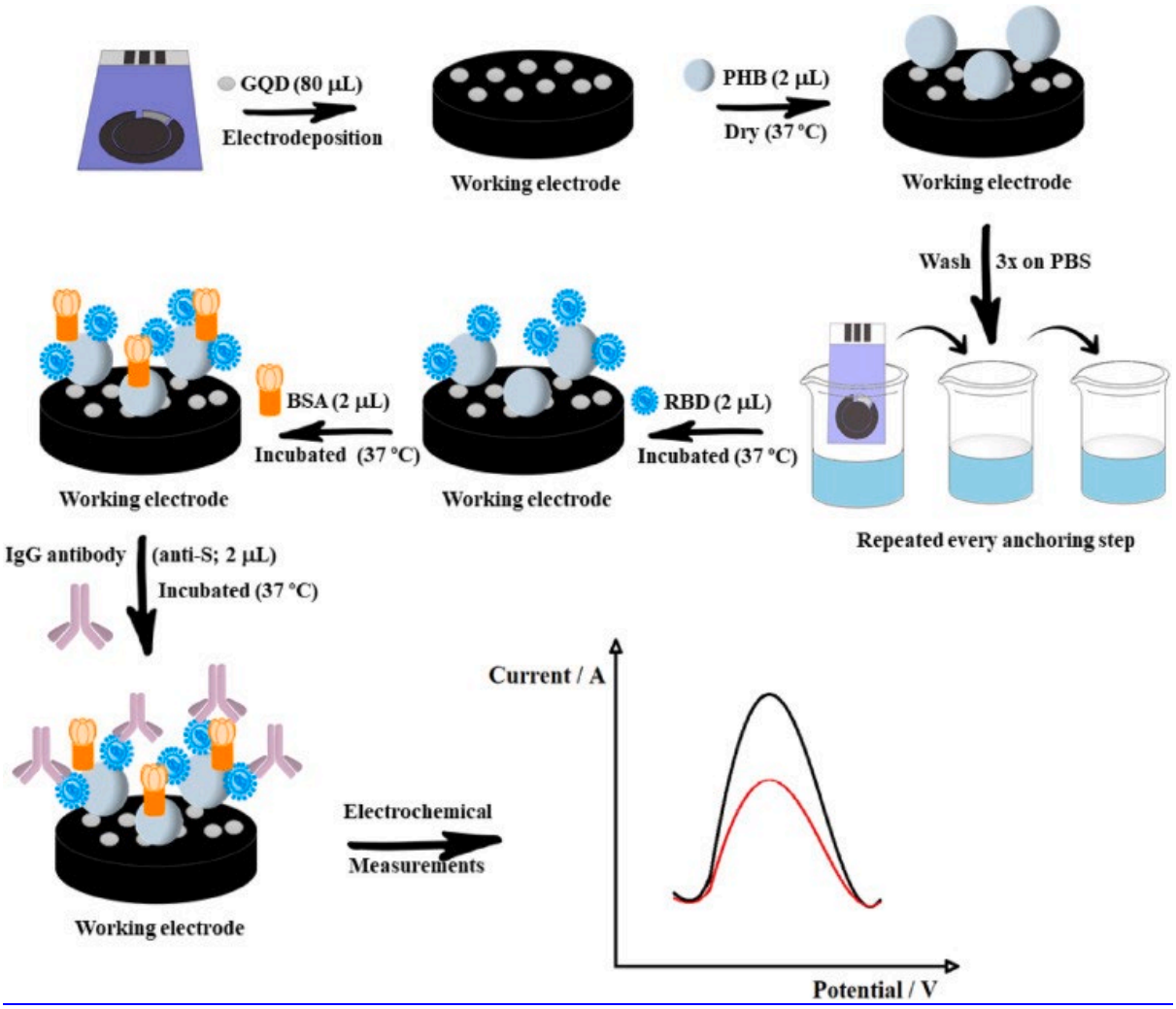

Scheme 1

Immunosensor step by step build-up.

2.6. Selectivity, analytical curve and sample analysis

Positive and negative (IgG) human serum samples were obtained from local hospital laboratories. Use of human samples was ethically assessed and approved by the Committee on Research Ethics, protocol number 30342520.5.0000.0008.

Human serum samples were 1000 × diluted on PBS solution. The diluted serum samples were added to W.E. (2 µL), incubated for 60 min at 37 °C and sequentially washed. Electrochemical signals were measured before and after incubation. Selectivity assay were performed with 1000 × diluted negative serum samples. Negative samples were spiked with AbS and YF antibodies (0.47 and 1.6 µg mL^{-1} final concentration, respectively). Two analytical curves were performed one on 0.1 mol L^{-1} PBS and another on 1000 × diluted negative human serum sample spiked with AbS (ranging from 25 µg mL^{-1} to 50 ng mL^{-1}, final concentration).

3. Results and discussions

3.1. GQD synthesis, characterization and immunosensor construction

PHB is a polymer produced by microorganisms as a form of energy storage [25]. PHB particles has shown stable interaction with biomolecules and also can be bioengineered to express specific

ligands to allow a specific interaction with biostructures. Here, PHB particles were used to modify the electrode surface and interact with SARS-CoV-2 RBD domain from the Spike protein (S1+S2 structure) one step later to create the selective layer.

GQD synthesis was carried out as described by Gevaerd et al. [26]. Synthesized nanoparticles were evaluated through FTIR to verify functional groups. Each step of immunosensor assemble was characterized by CV, SEM and EDS to evaluate material morphology and electrode surface after each modification. FTIR, SEM/EDS images and electrochemical behavior of the electrode with GQD, PHB and proteins are presented in Fig. S1A (FTIR) and S1C (SEM/EDS) and discussed in supplementary material (Section S1).

Fig. S1B shows $K_3[Fe(CN)_6]$ voltammetric behavior recorded after each modification. After GQD electrodeposition, the redox signal intensified from 7.98 µA to 12.09 µA (ΔI = 4.11 µA ± 3.8%, n = 3) as a result of GQD properties. GQD use in this system resides as current amplificator and also creates an anchoring interface between the SPE surface and PHB, through interaction with its highly functionalized surface. GQD PHB was subsequently added by drop-casting 2.0 µL (8.33 µg mL^{-1}) and dried at 37 °C. Comparing PHB behavior with GQD modified electrode, I_{pa} increased from 12.09 to 15.15 µA (ΔI = 3.06 ± 6.5%, n = 3), suggesting that PHB was successfully immobilized on the electrode surface. Observed ΔI_{pa} may be associated to GQD rearrangement due to an interaction with PHB, thus a larger electroactive area is available and a higher I_{pa} is registered. Next step consisted of anchoring RBD upon PHB, since the polymer particles self-assemble to proteins expressed with the SBD domain, already described in the literature [22], the incubation step can be performed. Therefore, 2.0 µL of RBD solution (0.47 µg mL^{-1}) was added to the WE surface and incubated in a water-saturated atmosphere at 37 °C. This condition allows the incubation to be carried out at 37 °C as it prevents the protein solution to dry and favors binding kinetics without compromising protein conformation. After incubating, the electrode was washed 3 times by immersion in PBS solution and CV measurements were performed. CV recorded after RBD anchoring displays a decrease in I_{pa} (ΔI = −2.36 ± 4.7%, n = 3), due to the hindering effect caused by protein binding over the PHB. Thus, RBD compromises electroactive area, as it is an insulator.

Last step consisted of blocking remaining active sites that RBD did not occupy. For this purpose, BSA (2.0 µL, 1.0 mg mL^{-1}) was anchored. BSA binds to such active sites, ensuring that the interaction of antibodies with the device may only occur by binding with RBD. The anchoring process was evaluated by the decrease of redox probe signals, since BSA causes an insulating effect, as can be seen on the CV.

The detection of IgG antibodies is based on the interaction between AbS and RBD, anchored at the electrode surface, thus forming the immunocomplex RBD-AbS. The RBD-AbS complex creates not just an insulating effect, but even a steric impediment, which affects the interaction between the redox probe and the electrode surface, leading to a decrease in the faradaic signal. Therefore, CV measurements showed a reduction of I_{pa} (ΔI = −2.66 ± 16.7%, n = 3), as shown in Fig. S1B –BSA-AbS. Each step was also evaluated through EIS, Fig. S2, and shows ΔR_{ct} concordant with CV data. Through the fit of equivalent circuit shown at Fig. S2, R_{ct} values were calculated and found to be 3.43 kΩ for bare electrode; 2.29 kΩ after GQD electrodeposition; 1.58 kΩ for PHB adsorption; 3.5 kΩ for anchoring RBD process; 4.7 kΩ after BSA and 6.1 kΩ to AbS detection and immunocomplex formation.

Alternatively, it was evaluated the construction of the immunosensor by exploring a single-step approach after GQD electrodeposition. In order to demonstrate this feature, a mixture of PHB, RBD and BSA was prepared under the same conditions previously applied. The device was step by step

evaluated by CV (Fig. S3A). GQD was electrodeposited, followed by drop-casting PHB-RBD-BSA mixture and dried at 37 °C. A decrease of I_{pa} is observed from the comparison of GQD voltammetric behavior and the mixture, better evidenced in Fig. S3B. The decrease is attributed to the mixture immobilization and its protein constituents, which partially blocks the electroactive surface. AbS detection was also evaluated and showed a decrease in I_{pa} due to the immunocomplex formation, as the main factor of steric impediment and resistance to charge transfer.

For comparison purposes, the same electrochemical experiments and anchoring were performed with EDC/NHS, a well-known crosslinking agent [27] for binding proteins (Fig. S3C). The overall build-up of the device shows similar electrochemical behavior to PHB (Fig. S3D). The proposed method was optimized, aiming to enhance the sensibility, reproducibility and feasibility of the sensor. Parameters involving the immunosensor assemble like GQD electrodeposition, modification with PHB and RBD immobilization (time and concentration), were evaluated. Tested and optimized parameters are summarized and discussed in supplementary material (Section S2).

3.2. Analytical performance, effect of matrix, selectivity and sample analysis

To evaluate how the optimized sensor responds to different target antibody concentrations, the proposed immunosensor was subjected to incubation with SARS-Cov-2 antibodies between 25 µg mL^{-1} and 50 ng mL^{-1} in PBS solution (Fig. 1). In order to verify the matrix effect on voltammetric response, a similar experiment was carried out using 1000x diluted human serum sample (negative) spiked with different AbS concentrations (Fig. 1).

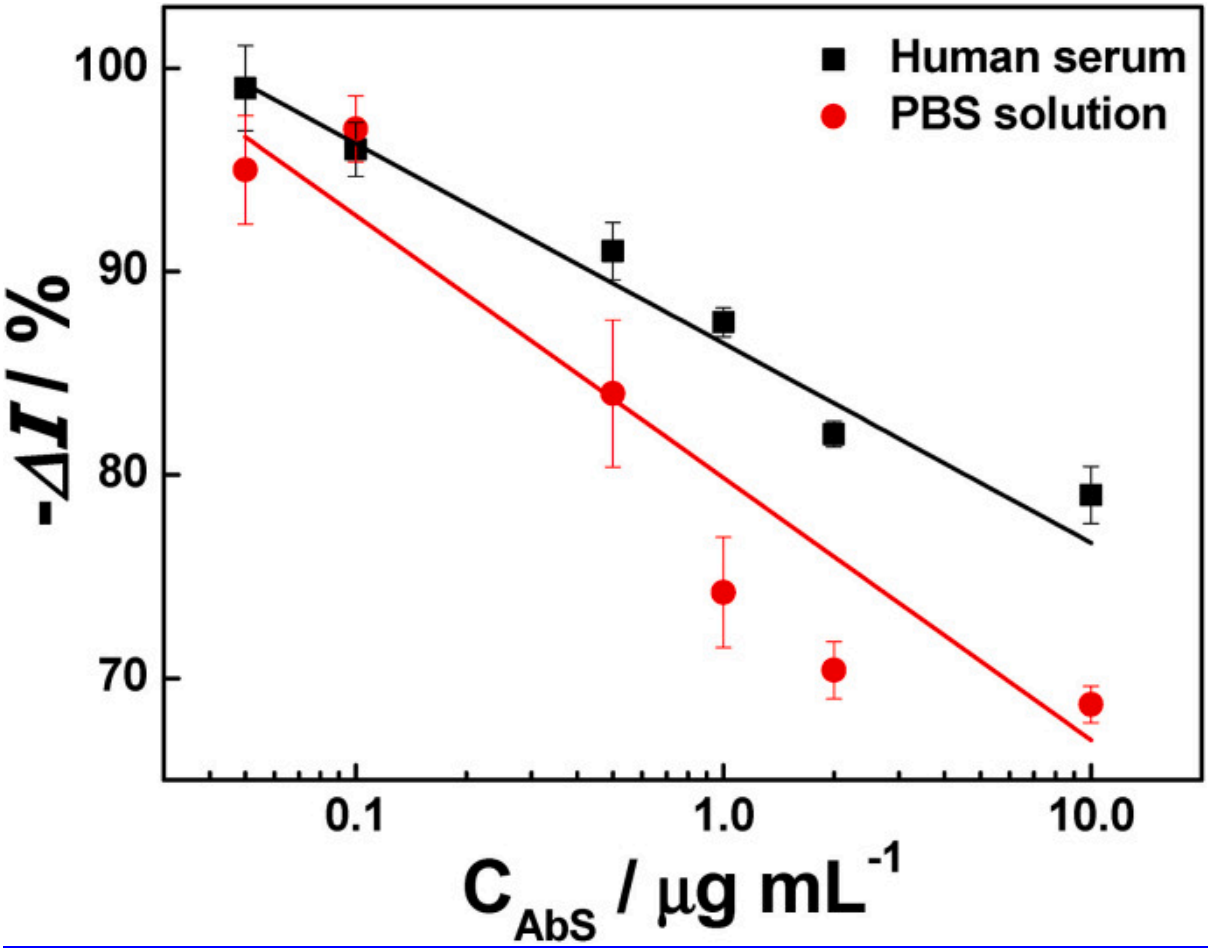

Fig. 1

Correlation curves representing probe current peak intensity vs antibody concentration (C_{AbS}) (n = 5, ±SD) obtained on 0.1 mol L^{-1} PBS medium and 1000x diluted negative serum sample.

For both studies, a relationship was observed between the decrease of faradaic signal and AbS concentration from 100 ng mL^{-1} to 10 µg mL^{-1} (ΔI_{serum} (%) = 86.47–9.80 log(C_{AbS}) and (ΔI_{PBS} (%) = 78.86–12.89 log(C_{AbS})). LOD was set as the lowest detectable value for both curves, 100 ng mL^{-1}. In addition, measurements recorded with AbS 25 µg mL^{-1} did not show variation in the voltammetric signal. This behavior can be related to the hook effect, which is a phenomenon whereby the effectiveness of antibodies to interact and form an immunocomplex is impaired when the concentration of an antibody or antigen is very high. Thus, the formation of immunocomplexes is lowered with higher concentrations [28,29]. The correlation curve obtained by fortified PBS solution showed a higher sensitivity to AbS detection compared to the human serum sample (Fig. 1). A sensibility around 10% lower using human serum was observed when compared to PBS solution. A crucial step for diagnostics through electrochemical measurements is the response in sample conditions since the complexity of the matrix can lead to unspecific interactions resulting in a false-positive diagnosis. The results suggested a slight effect on the response, which was not considered a drawback for the proposed immunosensor since the biological sample used is a very complex matrix.

Here, the combination of GQD and PHB as platforms to anchor protein and/or other biological components should be highlighted since it is a quick and feasible way to construct immunosensors. Overall performance and assembly time of GQD-PHB system is comparable with literature, which highlights the competitiveness of application when comparing to well-established methodologies. Table 1 summarizes other reports aimed at detecting COVID using well-known strategies for sensor preparation.

Table 1

Relevant papers using electrochemical methods for the diagnosis of SARS-CoV-2 infection.

Anchoring System	**Target**	**LOD**	**Sample**	**Assembly Time**	**Ref.**
SPAuE-Peptide	S-Protein	18.2 ng mL^{-1}	Nasopharyngeal swab	120 min.	[30]
Au-Anti-RBD	S-Protein	0.1 mg mL^{-1}	Human serum	1–3 days	[31]
Graphene – *Anti*-S-RBD	*Anti*-S (IgG/IgM)	ND	Blood and saliva	315 min.	[32]
NCM	Biotinylated Antibody (SARS-COV-2)	0.77 ng mL^{-1}	Buffer solution	240 min.	[33]
SPCE-NCM	*Anti*-N (IgG)	2 ng mL^{-1}	Human blood	60 min	[34]
SPE-CB	S/N Protein	19 and 8 ng mL^{-1}	Saliva	90 min.	[35]

Anchoring System	**Target**	**LOD**	**Sample**	**Assembly Time**	**Ref.**
Co–TiO_2 nanotubes	S-protein	14 nM	Nasopharyngeal and saliva	N.D.	[36]
ePAD-GO	*Anti*-S (IgG/IgM)	0.11 ng mL^{-1}	Human serum	180 min.	[37]
SPE-GQD-PHB	*Anti*-S (IgG)	100 ng mL^{-1}	Human serum	120 min.	This Work

Stencil printed carbon electrode – SPCE; Screen-printed Au Electrode – SPAuE; Nitrocelullose membrane – NCM; Screen printed electrode – SPE; Polyhydroxibutirate – PHB; Graphene Quantum Dots – GQD; Carbon Black – CB; Graphene oxide – GO; electrochemical paper-based analytical device – ePAD.

Selectivity is one of the top requirements for immunosensors, with false positives being a common hurdle to overcome in most diagnostic methods. The selectivity of the proposed sensor was tested against YF antibodies, as a control, and compared with the detection of the intended *Anti*-S antibodies, with YF antibodies as an interferent as well. The signal obtained before and after the interaction with each antibody and the comparison between the two procedures is shown at Fig. 2 A.

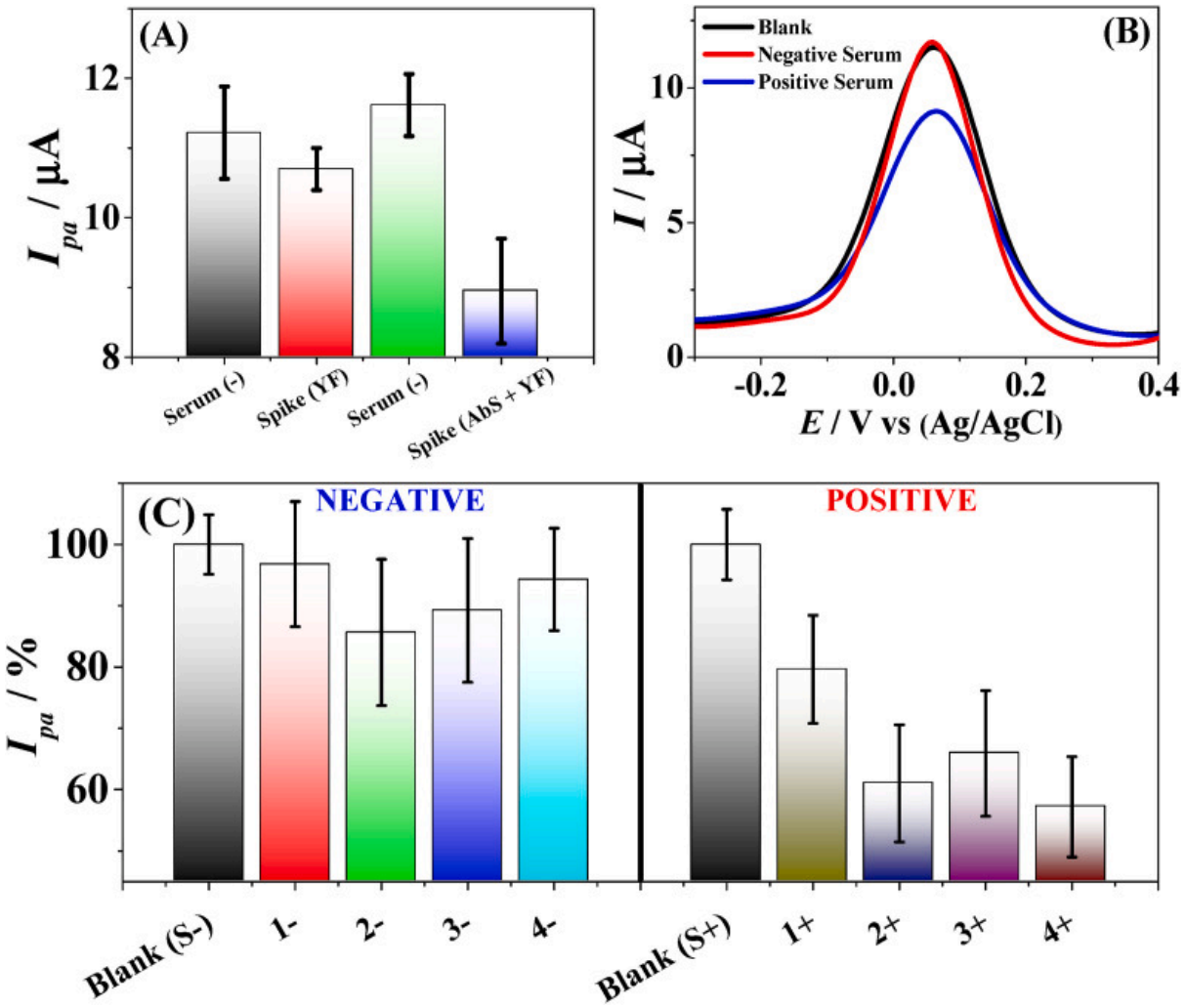

Fig. 2

(A) DPV data summarized for selectivity assay on negative serum sample against YF antibodies (n = 5, ±SD). (B) Representative DPV measurements obtained for positive and negative serum sample assays. (C) Summarized DPV assays for negative and positive human serum assays (n = 5, ±SD).

As observed in Fig. 2A, there is no statistical difference between the signal obtained before and after incubation of control antibodies (YF) ($t_{calculed} - 1.243 \leq 2.776 - t_{critic}$). This result indicates that the selective layer on the electrode surface did not interact with unspecific antibodies or YF. Fig. 2A also shows the signal before and after the incubation with both antibodies (AbS and YF - control), which AbS has provide a shift in the signal, implying an interaction with the device (RBD). In contrast, YF antibodies show no competition or interference for the detection.

The proposed sensor showed low interaction with the sample matrix, that paired with the good selectivity tested beforehand, allowed to differentiate 0.50 µg mL^{-1} of specific SARS-CoV-2 antibodies from a negative serum sample. Despite the number of antibodies in samples being dependent on the patient immune system and the chronology of the disease, varying through a wide range, the use of the GQD-PHB-RBD sensor can help diagnose the early onset of the Covid-19 disease.

Once the proposed sensor showed good selectivity, it was tested against positive and negative human serum samples (1000x diluted). Fig. 2B shows representative DPV measurements carried out

using the proposed immunosensor. Overall negative serum samples measurements did not alter the redox signal, while COVID-19 positive serum samples decreased I_{pa}. An overview of 8 serum samples analysis is summarized in Fig. 2C. Negative serum samples did not show a statistical difference from the blank signal ($t_{calculed} < t_{critic}$ 2.306). However, negative serum sample 2- has shown a slight statistical difference ($t_{calculed}$ 2.35 > t_{critic} 2.306), indicating a false positive test. Meanwhile, positive serum samples showed a difference ($t_{calculated} > t_{critic}$ 2.306) for all samples analyzed, clearly differentiating positives from negatives. Using eight serum samples, only one false positive and no false negatives were obtained. Thus, around 87.5% of samples investigated provided adequate results, but a more significant sample set should be evaluated to determine the device's effectiveness and its reliability as a point-of-care technique for diagnosing COVID-19. In addition, stability of response was evaluated considering immunosensor built and RBD-PHB dispersion. It was observed good performance for at least one week with the sensor “ready-to-use” and one month for solution.

4. Conclusion

The use of PHB showed potential for developing biosensors, as it is cheap, easy to obtain and can be scaled to industrial production. Its application relies on the self-assembly of proteins over its structure and the synergistic effect of biocompatibility, with no toxicity. In the present study, PHB showed better results than the traditional EDC/NHS protein coupling reaction. There were enhancements in electrode preparation time and the possibility of developing an immunosensor in a single drop since the proteins can be anchored prior to the electrode modification step. The proposed sensor showed selectivity against Yellow Fever antibodies and could differentiate COVID-19 negative from positive serum samples with results comparable with the literature. Thus, PHB grants a simpler array and has great potential for developing electrochemical biosensors, as demonstrated here for SARS-CoV-2.

CRediT authorship contribution statement

Gustavo Martins: Conceptualization, Formal analysis, Investigation, Methodology, Validation, Writing – original draft. **Jeferson L. Gogola:** Conceptualization, Methodology, Investigation. **Lucas H. Budni:** Investigation. **Maurício A. Papi:** Investigation. **Maritza A.T. Bom:** Methodology, Investigation. **Maria L.T. Budel:** Methodology, Investigation. **Emanuel M. de Souza:** Supervision, Resources, Funding acquisition, Writing – review & editing. **Marcelo Müller-Santos:** Supervision, Resources, Funding acquisition, Writing – review & editing. **Breno C.B. Beirão:** Supervision, Resources, Funding acquisition, Writing – review & editing. **Craig E. Banks:** Resources, Writing – review & editing. **Luiz H. Marcolino-Junior:** Conceptualization, Resources, Funding acquisition, Supervision, Writing – review & editing. **Márcio F. Bergamini:** Conceptualization, Resources, Funding acquisition, Supervision, Writing – review & editing.

Declaration of competing interest

The authors declare that they have no known competing financial interests or personal relationships that could have appeared to influence the work reported in this paper.

Acknowledgments

The authors acknowledge the financial support by CNPq (grants 408309/2018-0; 311290/2020-5, 309803/2020-9 and 402195/2020-5). This study was financed in part by the Coordenação de Aperfeiçoamento de Pessoal de Nível Superior – Brasil (CAPES) – Projects 1) Finance Code 001, NENNAM (PRONEX, Fund. Araucária/CNPq); 2) Grant number 88881.505280/2020–01; and FINEP.

Biographies

•

Gustavo Martins completed his MSc. at Federal University of Paraná, Brazil in 2018. The subject of his research was a development of a biochar based electrochemical immunosensor. Currently he is working with the development of 3D-printed electrochemical sensors and immunosensors.

•

Jeferson Luiz Gogola completed his MSc. at Federal University of Paraná, Brazil in 2018. The subject of his research was a development of a gold based immunosensor for the recognition of anti-Hantavirus Nucleoprotein. Currently he is working with the development of immunosensors aiming emerging diseases.

•

Lucas H. Budni is a chemistry undergraduate student at Federal University of Paraná, Brazil. He is now on internship under supervision of Prof. Dr. Márcio Bergamini, working on the development of immunosensors.

•

Maurício A. Papi: received his Ph. D. degree at Federal University of Paraná (UFPR) Brazil, in 2017, where he is currently a Postdoctoral Researcher. His research interests include the development and characterization of new nanostructured electrode materials and the development of miniaturized devices with electrochemical response for application in the environmental, health, food, and pharmaceutical areas.

•

Maritza A. T. Bom is graduated in Biomedicine with qualification in clinical analysis. MSc and PhD degree in Biochemistry from Federal University of Paraná (UFPR). Currently, as a technological development grant from CNPq, she has been dedicated to the development of a vaccine against COVID-19 using polyhydroxybutyrate nanoparticles.

•

Maria L. T. Budel is graduated in Biological Sciences from the Federal University of Paraná since 2020. Currently a CAPES Master's Scholar from the Graduate Program in Biochemistry Sciences, working with molecular biology and microorganism biotechnology.

•

Emanuel M. de Souza completed his degree in Pharmacy and Biochemistry from the Federal University of Paraná (1984) and a PhD in Science (Biochemistry) from the Federal University of Paraná (1990). He is currently a Full Professor at the Federal University of Paraná with experience in the field of Biochemistry, with an emphasis on Molecular Biology. He works mainly on the following topics: biological nitrogen fixation, regulation of gene expression in Azospirillum brasilense and Herbaspirillium seropedicae, expression and purification of proteins in *E. coli* and molecular mechanisms of plant-bacteria interaction.

•

Marcelo Müller-Santos has experience in the field of Biochemistry and Molecular Biology of Microorganisms. In recent years he has studied the metabolite of polyhydroxyalkanoates in bacteria and has been initiated projects in the areas of metabolic engineering and synthetic biology for the development of tools for the gene manipulation of gram-negative bacteria related with plants.

•

Breno C. B. Beirão completed Veterinary Medicine degree from the Federal University of Paraná (2009) and a master's degree in Microbiology, Parasitology and Pathology from the Federal University of Paraná (2011). He completed a PhD at the Roslin Institute / University of Edinburgh. He works mainly on the following subjects: immune system, flow cytometry, molecular biology, basic and applied immunology, production of therapeutic monoclonal antibodies.

•

Craig E. Banks is a professor of Chemistry at Manchester Metropolitan University and has elected as a highly cited researcher by Thomson Reuters; Listed in the World's Most Influential Scientific Minds 2014. His current research is directed toward the pursuit of studying the fundamental understanding and applications of nano-electrochemical systems such as graphene, carbon nanotube and nanoparticle derived sensors and developing novel electrochemical sensors via screen printing and related techniques.

•

Luiz Humberto Marcolino Junior received his Ph.D. degree in Analytical Chemistry from Federal University of São Carlos (UFSCar), Brazil, in 2007. He is a Professor in the Chemistry Department at Federal University of Paraná (DQ-UFPR), Curitiba-PR, Brazil. His current research interests are development of electrochemical sensors using nanostructured materials and development of microfluidic devices with electrochemical detection.

•

Márcio Fernando Bergamini received his Ph.D. degree in Analytical Chemistry in 2007 from Universidade Estadual Paulista (UNESP), Araraquara-SP, Brazil. He is currently Professor of Chemistry at Federal University of Paraná (UFPR). His principal research interest comprises the development of new electrochemical sensor for the determination of inorganic and organic compounds in pharmaceutical, biological or environmental samples.

Footnotes

Appendix A Supplementary data to this article can be found online at https://doi.org/10.1016/j.aca.2022.340442.

Data availability

No data was used for the research described in the article.

References

1. Kevadiya B.D., Machhi J., Herskovitz J., Oleynikov M.D., Blomberg W.R., Bajwa N., Soni D., Das S., Hasan M., Patel M., Senan A.M., Gorantla S., McMillan J.E., Edagwa B., Eisenberg R., Gurumurthy C.B., Reid S.P.M., Punyadeera C., Chang L., Gendelman H.E. Diagnostics for SARS-CoV-2 infections. *Nat. Mater.* 2021;20:593–605. doi: 10.1038/s41563-020-00906-z. [PMC free article] [PubMed] [CrossRef] [Google Scholar]

2. La Marca A., Capuzzo M., Paglia T., Roli L., Trenti T., Nelson S.M. Testing for SARS-CoV-2 (COVID-19): a systematic review and clinical guide to molecular and serological in-vitro diagnostic assays. *Reprod. Biomed. Online.* 2020;41:483–499. doi: 10.1016/j.rbmo.2020.06.001. [PMC free article] [PubMed] [CrossRef] [Google Scholar]

3. Jacot D., Moraz M., Coste A.T., Aubry C., Sacks J.A., Greub G., Croxatto A. Evaluation of sixteen ELISA SARS-CoV-2 serological tests. *J. Clin. Virol.* 2021;142 doi: 10.1016/j.jcv.2021.104931. [PMC free article] [PubMed] [CrossRef] [Google Scholar]

4. Pickering S., Batra R., Merrick B., Snell L.B., Nebbia G., Douthwaite S., Reid F., Patel A., Kia Ik M.T., Patel B., Charalampous T., Alcolea-Medina A., Lista M.J., Cliff P.R., Cunningham E., Mullen J., Doores K.J., Edgeworth J.D., Malim M.H., Neil S.J.D., Galão R.P. Comparative performance of SARS-CoV-2 lateral flow antigen tests and association with detection of infectious virus in clinical specimens: a single-centre laboratory evaluation study. *Lancet. Microbe.* 2021;2:e461–e471. doi: 10.1016/s2666-5247(21)00143-9. [PMC free article] [PubMed] [CrossRef] [Google Scholar]

5. Trombetta B.A., Kandigian S.E., Kitchen R.R., Grauwet K., Webb P.K., Miller G.A., Jennings C.G., Jain S., Miller S., Kuo Y., Sweeney T., Gilboa T., Norman M., Simmons D.P., Ramirez C.E., Bedard M., Fink C., Ko J., De León Peralta E.J., Watts G., Gomez-Rivas E., Davis V., Barilla R.M., Wang J., Cunin P., Bates S., Morrison-Smith C., Nicholson B., Wong E., El-Mufti L., Kann M., Bolling A., Fortin B., Ventresca H., Zhou W., Pardo S., Kwock M., Hazra A., Cheng L., Ahmad Q.R., Toombs J.A., Larson R., Pleskow H., Luo N.M., Samaha C., Pandya U.M., De Silva P., Zhou S., Ganhadeiro Z., Yohannes S., Gay R., Slavik J., Mukerji S.S., Jarolim P., Walt D.R., Carlyle B.C., Ritterhouse L.L., Suliman S. Correction to: evaluation of serological lateral flow assays for severe acute respiratory syndrome coronavirus-2. *BMC Infect. Dis.* 2021;1(580):21. doi: 10.1186/s12879-021-06257-7. BMC Infect. Dis. 21 (2021). doi:10.1186/s12879-021-06333-y. [PMC free article] [PubMed] [CrossRef] [Google Scholar]

6. Bordbar M.M., Samadinia H., Sheini A., Aboonajmi J., Sharghi H., Hashemi P., Khoshsafar H., Ghanei M., Bagheri H. A colorimetric electronic tongue for point-of-care detection of COVID-19 using salivary metabolites. *Talanta.* 2022;246 doi: 10.1016/j.talanta.2022.123537. [PMC free article] [PubMed] [CrossRef] [Google Scholar]

7. Parvin S., Hashemi P., Afkhami A., Ghanei M., Bagheri H. Simultaneous determination of BoNT/A and/E using an electrochemical sandwich immunoassay based on the nanomagnetic immunosensing platform. *Chemosphere.* 2022;298 doi: 10.1016/j.chemosphere.2022.134358. [PubMed] [CrossRef] [Google Scholar]

8. Khanmohammadi A., Aghaie A., Vahedi E., Qazvini A., Ghanei M., Afkhami A., Hajian A., Bagheri H. Electrochemical biosensors for the detection of lung cancer biomarkers: a review. *Talanta.* 2020;206 doi: 10.1016/j.talanta.2019.120251. [PubMed] [CrossRef] [Google Scholar]

9. Hashemi P., Afkhami A., Baradaran B., Halabian R., Madrakian T., Arduini F., Nguyen T.A., Bagheri H. Well-orientation strategy for direct immobilization of antibodies: development of the immunosensor using the boronic acid-modified magnetic graphene nanoribbons for ultrasensitive detection of lymphoma cancer cells. *Anal. Chem.* 2020;92:11405–11412. doi: 10.1021/acs.analchem.0c02357. [PubMed] [CrossRef] [Google Scholar]

10. Cho I.H., Kim D.H., Park S. Electrochemical biosensors: perspective on functional nanomaterials for on-site analysis. *Biomater. Res.* 2020;24 doi: 10.1186/s40824-019-0181-y. [PMC free article] [PubMed] [CrossRef] [Google Scholar]

11. Hassanvand Z., Jalali F., Nazari M., Parnianchi F., Santoro C. Carbon nanodots in electrochemical sensors and biosensors: a review. *Chemelectrochem.* 2021;8:15–35. doi: 10.1002/celc.202001229. [CrossRef] [Google Scholar]

12. Wang S., Cole I.S., Li Q. The toxicity of graphene quantum dots. *RSC Adv.* 2016;6:89867–89878. doi: 10.1039/c6ra16516h. [CrossRef] [Google Scholar]

13. Bressi V., Ferlazzo A., Iannazzo D., Espro C. Graphene quantum dots by eco-friendly green synthesis for electrochemical sensing: recent advances and future perspectives. *Nanomaterials.* 2021;11 doi: 10.3390/nano11051120. [PMC free article] [PubMed] [CrossRef] [Google Scholar]

14. Gogola J.L., Martins G., Gevaerd A., Blanes L., Cardoso J., Marchini F.K., Banks C.E., Bergamini M.F., Marcolino-Junior L.H. Label-free aptasensor for p24-HIV protein detection based on graphene quantum dots as an electrochemical signal amplifier. *Anal. Chim. Acta.* 2021;1166 doi: 10.1016/j.aca.2021.338548. [PubMed] [CrossRef] [Google Scholar]

15. Tabish T.A., Hayat H., Abbas A., Narayan R.J. Graphene quantum dots-based electrochemical biosensing platform for early detection of acute myocardial infarction. *Biosensors.* 2022;12 doi: 10.3390/bios12020077. [PMC free article] [PubMed] [CrossRef] [Google Scholar]

16. Parlane N.A., Rehm B.H.A., Wedlock D.N., Buddle B.M. Novel particulate vaccines utilizing polyester nanoparticles (bio-beads) for protection against Mycobacterium bovis infection-A review. *Vet. Immunol. Immunopathol.* 2014;158:8–13. doi: 10.1016/j.vetimm.2013.04.002. [PubMed] [CrossRef] [Google Scholar]

17. Parlane N.A., Grage K., Mifune J., Basaraba R.J., Wedlock D.N., Rehm B.H.A., Buddle B.M. Vaccines displaying mycobacterial proteins on biopolyester beads stimulate cellular immunity and induce protection against tuberculosis. *Clin. Vaccine Immunol.* 2012;19:37–44. doi: 10.1128/CVI.05505-11. [PMC free article] [PubMed] [CrossRef] [Google Scholar]

18. Martínez-Donato G., Piniella B., Aguilar D., Olivera S., Pérez A., Castañedo Y., Alvarez-Lajonchere L., Dueñas-Carrera S., Lee J.W., Burr N., Gonzalez-Miro M., Rehm B.H.A. Protective T cell and antibody immune responses against hepatitis C virus achieved using a biopolyester-bead-based vaccine delivery system. *Clin. Vaccine Immunol.* 2016;23:370–378. doi: 10.1128/CVI.00687-15. [PMC free article] [PubMed] [CrossRef] [Google Scholar]

19. Parlane N.A., Gupta S.K., Rubio-Reyes P., Chen S., Gonzalez-Miro M., Wedlock D.N., Rehm B.H.A. Self-assembled protein-coated polyhydroxyalkanoate beads: properties and biomedical applications. *ACS Biomater. Sci. Eng.* 2017;3:3043–3057. doi: 10.1021/acsbiomaterials.6b00355. [PubMed] [CrossRef] [Google Scholar]

20. Soda N., Gonzaga Z.J., Chen S., Koo K.M., Nguyen N.T., Shiddiky M.J.A., Rehm B.H.A. Bioengineered polymer nanobeads for isolation and electrochemical detection of cancer biomarkers. *ACS Appl. Mater. Interfaces.* 2021;13:31418–31430. doi: 10.1021/acsami.1c05355. [PubMed] [CrossRef] [Google Scholar]

21. Chiellini E., Errico C., Bartoli C., Chiellini F. Poly(hydroxyalkanoates)-based polymeric nanoparticles for drug delivery. *J. Biomed. Biotechnol.* 2009;2009 doi: 10.1155/2009/571702. [PMC free article] [PubMed] [CrossRef] [Google Scholar]

22. Lee S.J., Park J.P., Park T.J., Lee S.Y., Lee S., Park J.K. Selective immobilization of fusion proteins on poly(hydroxyalkanoate) microbeads. *Anal. Chem.* 2005;77:5755–5759. doi: 10.1021/ac0505223. [PubMed] [CrossRef] [Google Scholar]

23. Bertani G. Studies on lysogenesis I. *J. Bacteriol.* 1951;62:293–300. doi: 10.1128/jb.62.3.293-300.1951. [PMC free article] [PubMed] [CrossRef] [Google Scholar]

24. Bradford M. A rapid and sensitive method for the quantitation of microgram quantities of protein utilizing the principle of protein-dye binding. *Anal. Biochem.* 1976;72:248–254. doi: 10.1006/abio.1976.9999. [PubMed] [CrossRef] [Google Scholar]

25. Müller-Santos M., Koskimäki J.J., Alves L.P.S., De Souza E.M., Jendrossek D., Pirttilä A.M. The protective role of PHB and its degradation products against stress situations in bacteria. *FEMS Microbiol. Rev.* 2021;45 doi: 10.1093/femsre/fuaa058. [PubMed] [CrossRef] [Google Scholar]

26. Gevaerd A., Banks C.E., Bergamini M.F., Marcolino-Junior L.H. Graphene quantum dots modified screen-printed electrodes as electroanalytical sensing platform for diethylstilbestrol. *Electroanalysis.* 2019;31:838–843. doi: 10.1002/elan.201800838. [CrossRef] [Google Scholar]

27. Fischer M.J.E. Amine coupling through EDC/NHS: a practical approach. *Methods Mol. Biol.* 2010;627:55–73. doi: 10.1007/978-1-60761-670-2_3. [PubMed] [CrossRef] [Google Scholar]

28. Roy R.D., Rosenmund C., Stefan M.I. Cooperative binding mitigates the high-dose hook effect. *BMC Syst. Biol.* 2017;11 doi: 10.1186/s12918-017-0447-8. [PMC free article] [PubMed] [CrossRef] [Google Scholar]

29. Dodig S. Interferences in quantitative immunochemical methods. *Biochem. Med.* 2009;19:50–62. doi: 10.11613/bm.2009.005. [CrossRef] [Google Scholar]

30. Soto D., Orozco J. Peptide-based simple detection of SARS-CoV-2 with electrochemical readout. *Anal. Chim. Acta.* 2022 doi: 10.1016/j.aca.2022.339739. [PMC free article] [PubMed] [CrossRef] [Google Scholar]

31. Rashed M.Z., Kopechek J.A., Priddy M.C., Hamorsky K.T., Palmer K.E., Mittal N., Valdez J., Flynn J., Williams S.J. Rapid detection of SARS-CoV-2 antibodies using electrochemical impedance-based detector. *Biosens. Bioelectron.* 2021;171 doi: 10.1016/j.bios.2020.112709. [PMC free article] [PubMed] [CrossRef] [Google Scholar]

32. Torrente-Rodríguez R.M., Lukas H., Tu J., Min J., Yang Y., Xu C., Rossiter H.B., Gao W., SARS-CoV-2 RapidPlex A graphene-based multiplexed telemedicine platform for rapid and low-cost COVID-19 diagnosis and monitoring. *Matter.* 2020;3:1981–1998. doi: 10.1016/j.matt.2020.09.027. [PMC free article] [PubMed] [CrossRef] [Google Scholar]

33. Grant B.D., Anderson C.E., Williford J.R., Alonzo L.F., Glukhova V.A., Boyle D.S., Weigl B.H., Nichols K.P. SARS-CoV-2 coronavirus nucleocapsid antigen-detecting half-strip lateral flow assay toward the development of point of care tests using commercially available reagents. *Anal. Chem.* 2020;92:11305–11309. doi: 10.1021/acs.analchem.0c01975. [PMC free article] [PubMed] [CrossRef] [Google Scholar]

34. Samper I.C., Sánchez-Cano A., Khamcharoen W., Jang I., Siangproh W., Baldrich E., Geiss B.J., Dandy D.S., Henry C.S. Electrochemical capillary-flow immunoassay for detecting anti-SARS-CoV-2

nucleocapsid protein antibodies at the point of care. *ACS Sens.* 2021;6:4067–4075. doi: 10.1021/acssensors.1c01527. [PMC free article] [PubMed] [CrossRef] [Google Scholar]

35. Fabiani L., Saroglia M., Galatà G., De Santis R., Fillo S., Luca V., Faggioni G., D'Amore N., Regalbuto E., Salvatori P., Terova G., Moscone D., Lista F., Arduini F. Magnetic beads combined with carbon black-based screen-printed electrodes for COVID-19: a reliable and miniaturized electrochemical immunosensor for SARS-CoV-2 detection in saliva. *Biosens. Bioelectron.* 2021;171 doi: 10.1016/j.bios.2020.112686. [PMC free article] [PubMed] [CrossRef] [Google Scholar]

36. Vadlamani B.S., Uppal T., Verma S.C., Misra M. Functionalized tio2 nanotube-based electrochemical biosensor for rapid detection of sars-cov-2. *Sensors.* 2020;20:1–10. doi: 10.3390/s20205871. [PMC free article] [PubMed] [CrossRef] [Google Scholar]

37. Yakoh A., Pimpitak U., Rengpipat S., Hirankarn N., Chailapakul O., Chaiyo S. Paper-based electrochemical biosensor for diagnosing COVID-19: detection of SARS-CoV-2 antibodies and antigen, Biosens. *Bioelectron.* 2021;176 doi: 10.1016/j.bios.2020.112912. [PMC free article] [PubMed] [CrossRef] [Google Scholar]